

Use of 2-Aminopurine and Tryptophan Fluorescence as Probes in Kinetic Analyses of DNA Polymerase β [†]

Christopher A. Dunlap[‡] and Ming-Daw Tsai*

Departments of Chemistry and Biochemistry and Ohio State Biochemistry Program, The Ohio State University, Columbus, Ohio 43210

Received March 19, 2002; Revised Manuscript Received July 17, 2002

ABSTRACT: Although the use of 2-aminopurine (2-AP) as a probe in stopped-flow analyses of DNA polymerase β (Pol β) had provided important mechanistic insight, the conditions used were limited by the location of 2-AP and the use of a combination of tryptophan (Trp) and 2-AP fluorescence. This study examined different DNA substrates to identify several factors that can affect the observed signal in stopped-flow experiments. Both Trp and 2-AP emissions were separately excited and monitored. It was found that both probes show a fast phase and a slow phase of fluorescence changes, but the direction and the amplitude vary greatly between the two probes and between different DNA substrates. Detailed analyses suggested that the location of 2-AP in the template has a significant impact on the fluorescence properties of 2-AP and that a location opposite the incoming dNTP, which has been used in all such studies in the past, is not optimal. In particular, the results show that placing 2-AP one base after the templating base greatly enhances the signal intensity, which suggests a significant change in base stacking interactions at this position during nucleotide incorporation. These results allowed us to derive an improved set of conditions which were then used to reevaluate results from previous reports. It also allows greater freedom in the type of base pairs studied, since 2-AP is not the templating base in the nascent base pair. Kinetic constants were determined for dNTP and catalytic Mg^{2+} . The results obtained from stopped-flow experiments were compared to results from chemical quench. Stopped flow of incorrect dNTP incorporation and the reverse reaction are also reported, which provide useful information to the mechanism of Pol β .

Understanding how DNA polymerases control their substrate specificities has been the subject of extensive research, as described in several recent reviews (2–5). A two-metal ion mechanism has been proposed to be common for all families of nucleotide polymerases (6, 7). Among the large number of polymerases known to date, mammalian DNA polymerase β (Pol β)¹ is one of a few which lack intrinsic exonuclease activity and is thus an ideal model for studying the detailed mechanism of enzymatic DNA polymerization. It has been investigated extensively by X-ray crystallography (8–12), kinetic analyses (13–17), site-directed mutagenesis (1, 18–23), and stopped-flow studies (9, 21, 24, 25).

Earlier crystal structures of Pol β (8, 10, 11) show a large (subdomain-closing) conformational change upon binding Mg^{2+} ·dNTP and the catalytic Mg^{2+} . In our previous stopped-flow studies of Pol β , two phases of fluorescence change were observed (Figure 1A) (9, 24, 25). By using a chain-terminated primer DNA that prevents chemistry from oc-

curing, we have shown that the fast phase occurs before chemistry and the slow phase is limited by chemistry (Figure 1B). We assigned the fast phase to the subdomain-closing conformational change since stopped-flow results show that the fast phase is induced by binding of Cr(III)dNTP (25), and the intermediate crystal structure of the Pol β ·DNA·Cr(III)dNTP complex (the state prior to binding of the catalytic Mg^{2+}) obtained by us indicates that this complex already exists in the closed state (9). Since these results and interpretations contradicted the generally accepted theory that the catalysis of DNA polymerases involves a rate-limiting conformational change (2, 4, 11, 22), it is important to further evaluate the stopped-flow results with improved conditions.

Previous stopped-flow studies of Pol β used 2-aminopurine (2-AP), a fluorescent analogue of adenine and guanine, as a spectroscopic probe to observe conformational changes along the reaction pathway (9, 21, 24–26). In these assays, 2-AP serves as the template base, allowing a pseudo-Watson–Crick base pair to be formed upon the addition of TTP or dCTP. Stopped-flow studies employing 2-AP at this location suffer many limitations: (i) under these conditions, only the incorporation of pyrimidines can be examined; (ii) the study of purine incorporation and pyrimidine–pyrimidine mismatches are not possible; (iii) the use of a pseudo-Watson–Crick base pair (2-AP·T) is always open to criticism on the grounds that the results are not representative of a true Watson–Crick base pair (A·T); (iv) at the template base position, 2-AP does not provide the optimal signal-to-noise

[†] This work was supported by NIH Grant GM43268. This is paper 10 in the series DNA Polymerase β . For paper 9, see ref 1.

* To whom correspondence should be addressed at the Department of Chemistry [telephone (614) 292-3080; fax (614) 292-1532; e-mail tsai.7@osu.edu].

[‡] Department of Chemistry.

¹ Abbreviations: 2-AP, 2'-deoxy-2-aminopurine; dNTP, 2'-deoxy-nucleoside 5'-triphosphate; dATP, 2'-deoxyadenosine 5'-triphosphate; dCTP, 2'-deoxycytidine 5'-triphosphate; TTP, thymidine 5'-triphosphate; PP_i, pyrophosphate; Pol β , *Rattus norvegicus* DNA polymerase β ; Trp, tryptophan.

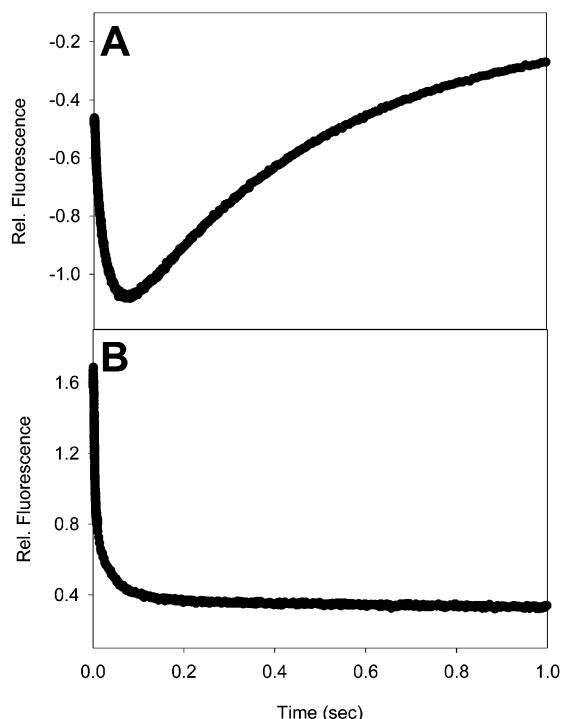


FIGURE 1: Stopped-flow fluorescence assays of Pol β taken from our previous study (9). (A) Incorporation of TTP opposite the template 2-aminopurine. One syringe contained 2 μ M Pol β preincubated with 0.6 μ M 20/36AP substrate and 5 mM MgCl₂. The other syringe contained 200 μ M TTP and 5 mM MgCl₂. (B) Incorporation of TTP opposite the template 2-aminopurine with ddAMP at the 3' end of the primer.

ratio, as determined in the current study. The location of 2-AP at the templating position in these studies was based on a similar assay used to examine the Klenow fragment and T4 DNA polymerase (26) and on the incorrect assumption that base pairing significantly influences the fluorescence of 2-AP. However, a closer review of the literature indicates that the fluorescence of 2-AP is only quenched slightly upon base pairing in an early study (27). On the other hand, enzyme binding to single- or double-stranded DNA can induce large increases in fluorescence (28), indicating that base stacking interactions can greatly influence the fluorescence of 2-AP. Several recent studies have examined base stacking interactions with 2-AP fluorescence for a variety of proteins (29–34). Analysis of Pol β crystal structures (11) suggests that alternate locations in the templating strand may undergo significant changes in base stacking during the course of nucleotide incorporation and may serve as a better reporter of conformational changes. Also, by placing 2-AP in an alternate location, additional base pairs and incorrect base pairs could be examined.

Another limitation in all our previous stopped-flow studies of Pol β is that the detection of fluorescence signals relied upon a combination of 2-aminopurine (2-AP) and tryptophan (Trp) fluorescence, since this offered the greatest signal-to-noise ratio under the reaction conditions (9, 21, 24, 25). An intermediate excitation wavelength (290 nm) was used (the excitation maxima are 312 nm for 2-AP and 285 nm for Trp), and all emission above 320 nm was collected (the emission maxima are 362 nm for 2-AP and 340 nm for Trp). Such conditions have the potential to complicate the analysis, if the two fluorophores do not report the same processes. For

example, a physical event may alter the fluorescence of one probe but not the other or may enhance the emission of one probe while quenching emission of the other.

As a continuation of our previous studies, this work examined the conditions for stopped-flow analyses, aiming at improving signal intensity and increasing the versatility of the dNTP studied. The results indicate that placing 2-AP one base below the nascent base pair results in a dramatic improvement in the signal-to-noise ratio and placing 2-AP two bases below the nascent base pair offers an acceptable signal-to-noise ratio and greater flexibility in the variety of base pairs that could be studied. These two conditions were then used to reinvestigate most of the stopped-flow experiments reported previously, including those of the incorrect dNTP and the reverse reaction.

MATERIALS AND METHODS

Materials. Ultrapure dNTPs and G-25 microspin columns were purchased from Pharmacia. Radiolabeled [γ -³²P]ATP was purchased from ICN biomedical. T4 polynucleotide kinase was obtained from New England Biolabs. C₁₈ cartridges were obtained from Waters Corp. All other chemicals used were obtained from Sigma-Aldrich. Pol β was purified as previously described (23) from an overexpressing *Escherichia coli* system, BL21(DE3)(plysS, pET17-Pol β). The enzyme concentration was determined by using a molar absorption coefficient of 21 200 M⁻¹ cm⁻¹ at 280 nm (35). The enzyme was estimated to be >95% homogeneous on the basis of SDS-PAGE analysis developed using the silver staining method (36).

DNA Substrates. Custom synthesized oligomers were purchased from Integrated DNA Technologies (Coralville, IA). The oligomers were further purified by 18% (w/v) polyacrylamide/7 M urea gels. The appropriate bands were identified by UV shadowing on a fluorescent TLC plate and excised from the gel. The gel fragments were extracted with 100 mM triethylamine acetate and 1 mM EDTA. The extract was subsequently desalted with a C₁₈ cartridge and eluted using methanol-water (60:40). After removal of the solvent with vacuum, the oligomers were resuspended in 50 mM KCl, and the concentration was determined by UV using a calculated molar absorption coefficient (37). The oligomers were then stored at -20 °C.

DNA substrates used in the chemical quench experiments were 5'-end labeled using T4 polynucleotide kinase and [γ -³²P]ATP (4500 Ci/mol) according to the manufacturer's protocol. Labeled DNA was separated from unreacted ATP and Mg²⁺ using a G-25 microspin column with a small amount of Chelex 100 resin added to it. The T4 polynucleotide kinase was inactivated by heating at 65 °C for 20 min. Substrate annealing was as follows: labeled primer was added to the appropriate unlabeled template, heated to 80 °C, and then slowly cooled to room temperature.

DNA substrates used in the stopped-flow experiments were mixed 1:1 (primer/template), then annealed by heating to 80 °C, and then slowly cooled to room temperature. Some substrates used in stopped-flow assays contained primers terminated with a dideoxynucleotide and are signified by a (dd) in their nomenclature (i.e., 18dd/36AP). The oligos terminated with a dideoxynucleotide were obtained commercially from Integrated DNA Technologies (Coralville, IA)

and were synthesized using standard phosphoramidite techniques.

Chemical Quench Experiments. A rapid quench instrument (KinTek Instrument Corp., State College, PA) was used for reaction times ranging from 5 ms to 20 s. Pol β and DNA were preincubated for 5 min before rapid mixing with dNTP and Mg^{2+} . The assay buffer used in all experiments contained 50 mM Tris, 50 mM KCl, 10% (v/v) glycerol, and 1 mM DTT, at pH 8.0. The typical assay was conducted at 37 °C using 100 nM DNA, 300 nM Pol β , and assay buffer at pH 8.0 and quenched using 300 mM EDTA (all final concentrations). The reaction products were then mixed 1:1 with formamide and loaded on an 18% (w/v) polyacrylamide/7 M urea gel. The disappearance of substrate and the formation of product were analyzed with a STORM 840 PhosphorImager (Molecular Dynamics). Assays were typically performed in triplicate and the results averages.

Stopped-Flow Fluorescence Assays. Experiments were performed on an Applied Photophysics SX 18MV stopped-flow apparatus. The excitation wavelengths were 285 and 315 nm for tryptophan and 2-aminopurine, respectively, with a spectral band-pass of 4 nm. Emission was monitored using a 340 nm band-pass filter (Corion, 10 nm) for tryptophan and a 360 nm high-pass filter (Corion) for 2-aminopurine. The assay buffer used in all experiments contained 50 mM Tris, 50 mM KCl, 10% (v/v) glycerol, and 1 mM DTT, at pH 8.0. A typical experiment would consist of the following: syringe A, 200 nM DNA with 2-AP in the template, 400 nM Pol β , assay buffer, and 8 mM $MgCl_2$ at pH 8.0 and 37 °C; syringe B, 400 μ M dNTP, 8 mM $MgCl_2$, and assay buffer at pH 8.0 and 37 °C. In every experiment, both syringes contained solutions with 10% glycerol to prevent problems related to viscosity. Nucleotide dependence experiments were performed with saturating Mg^{2+} (10 mM). Mg^{2+} dependence experiments were performed with saturating dNTP (300 μ M). All buffers were filtered with a 0.45 μ m filter and degassed prior to use. Typically, a minimum of 10 trials would be performed and averaged. For presentation purposes (easier to compare and visualize), some of the fluorescence profiles presented here were collected for 1 s with a sampling frequency of 1 kHz. Profiles were typically collected in dual time frame mode (with each time frame corresponding to the length of a given phase) with 500 data points in each time frame. The results for each case were the same.

Data Analysis. Data obtained from kinetic assays were fitted by nonlinear regression using Sigma Plot software (Jandel Scientific) with the appropriate equations. The apparent burst rate constant (k_{obs}) for each particular concentration of ligand (dNTP or Mg^{2+}) was determined by fitting the time courses for the formation of product with the equation:

$$[\text{product}] = A_1[1 - \exp(-k_{obs1}t)] + A_2[1 - \exp(-k_{obs2}t)] + \dots + C \quad (1)$$

where A represents the burst amplitude and C is an offset constant for stopped-flow experiments. The turnover number k_{max} and apparent dissociation constant for a ligand ($K_{d,app}$) were then obtained by plotting the rate constants (k_{obs}) against the ligand concentrations $[L]$ and fitting the data with the hyperbolic equation:

$$k_{obs} = k_{max}[L]/(K_{d,app} + [L]) \quad (2)$$

RESULTS AND DISCUSSION

Effects of the Location of 2-AP on the Stopped-Flow Analyses of Pol β Catalysis. A series of DNA substrates were produced as shown in Figure 2A. The template strand, a 36mer with 2-AP at position 16 (5'-3'), is the same as that used in previous studies (9, 21, 24, 25). The primer strand varies from 18 to 21 nucleotides, placing 2-AP at positions ranging from +2 to -1 relative to the nascent base pair. The resulting primer/template substrates are named 18/36AP, 19/26AP, 20/36AP, and 21/36AP, respectively. Figure 2B shows the relative location of 2-AP in the active site of Pol β for the various primer/template pairs.

These substrates were first subjected to stopped-flow analysis of nucleotide incorporation catalyzed by Pol β under conditions used previously, with the exception that both 2-AP and Trp emissions were separately excited and monitored, as described in the Materials and Methods section. Briefly, fluorescence emission is monitored as a function of time following rapid mixing of the Pol β -DNA complex with dNTP (with 8 mM Mg^{2+} present in both solutions). An enzyme:DNA ratio of 2:1 was chosen to form the Pol β -DNA complex. At this ratio, there is sufficient enzyme to reasonably saturate the DNA substrate (23) but limit the formation of a 2:1 complex (Pol β -DNA), which is known to occur and could possibly complicate the analysis (38, 39). Another consideration in choosing the enzyme:DNA ratio is the use of two fluorophores. While 2-AP is the primary fluorophore, Trp fluorescence is also desired. A large excess of Pol β would reduce the signal-to-noise ratio in the Trp experiments by adding a large fluorescence background. A compromise was made so that both fluorophores could be examined under identical conditions. Under these conditions DNA release (steady-state rates ~ 0.2 – 0.6 s $^{-1}$) is known to be much slower than product formation (~ 10 – 18 s $^{-1}$), allowing us to perform these experiments under single turnover conditions. These results are similar to those previously reported by our laboratory on similar primer/template substrates (23).

As shown in Figure 3, the results in most cases show two phases of time-dependent fluorescence change, consistent with previous results shown in Figure 1A. However, the four different DNA substrates give rise to very different signals for both 2-AP and Trp. Specifically affected are signal-to-noise ratios, direction of fluorescence change, and relative emission amplitudes of the two phases. In one case, the fluorescence change is so small as to be unobservable (Figure 3D). The most sensitive location in terms of the signal-to-noise ratio was the 19/36AP substrate (Figure 3B) with 2-AP fluorescence, offering an approximately 20-fold improvement over other conditions as explained in the legend. A comparison between the 19/36AP substrate and the 18/36AP substrate under the same conditions and scale is provided in the inset of Figure 3B. On the basis of previous analyses as described in the introduction and the updated kinetic scheme of Pol β as shown in Scheme 1 (9), the fast phase can be assigned to the change from the E·DNA binary complex (the open form) to the closed ternary complex E'·DNA·N or E'·DNA·N·M, where N represents $MgdNTP$ and M represents the catalytic Mg^{2+} . The slow phase reflects the events after

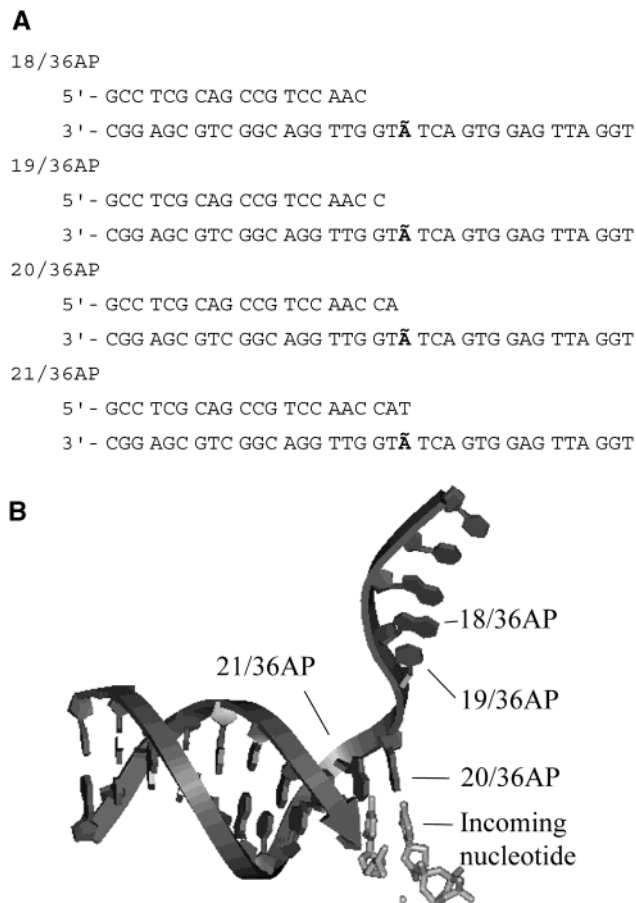


FIGURE 2: (A) Sequences of DNA substrates. \tilde{A} represents 2-aminopurine. (B) Relative location of 2-AP for the DNA substrates shown in (A). The conformation of DNA is based on the structure of DNA bound to Pol β (11).

the chemical step. In the rest of the paper, we describe additional experiments to show that the use of different substrates and different experimental conditions has led to confirmation of previous results from our laboratory and also provide additional insight in understanding the catalytic mechanism of Pol β .

New Insight from Trp Fluorescence. The rat Pol β used in our studies has only one tryptophan residue, Trp325, located 10 residues from the C-terminus. On the basis of crystal structures, this Trp residue is not directly involved in DNA or dNTP binding. It lies on the surface of the fingers subdomain [using the nomenclature of Steitz (40)], which undergoes a large conformational change upon dNTP binding. Thus it can serve as a reporter for conformational changes of the protein, but its fluorescence should be insensitive to the location of the 2-AP probe. As shown in Figure 3, in three of the four experiments (except 19/36AP in Figure 3B), the Trp fluorescence showed two phases of fluorescence change, a fast and decreasing phase followed by a slow and increasing phase similar to the curve shown in Figure 1A. In these three cases, a control experiment in which 2-AP was replaced in the template with adenosine showed the same result and verified that the Trp fluorescence was unaffected by the presence of 2-AP.

The Trp fluorescence of the 19/36AP experiment differs from those of the other experiments in that it shows two decreasing phases. It is also unique in that, in a control

experiment where 2-AP is replaced by adenosine, the amplitude of the second phase became smaller. The rate of the second phase is the same for both substrates ($\sim 15\text{ s}^{-1}$). We believe that this effect is caused by binding of the dNTP to the product of the reaction (in this case, 20/36AP) and forming the ternary complex of the mismatch (in this case, 2-AP \cdot A). To test this possibility, we performed separate stopped-flow assays with 20/36AP to study the incorporation of mismatched nucleotide dATP. As shown in Figure 4, the fluorescence decreases upon formation of the 2-AP \cdot A ternary complex, which occurs at a rate of $\sim 130\text{ s}^{-1}$, ca. 10 times faster than the formation of the 20/36AP product (the second phase of Figure 3B). On the other hand, the rate of formation of the next product (21/36AP, with 2-AP \cdot A mismatch) is very slow ($\sim 0.01\text{ s}^{-1}$), similar to that previously reported (24). It is important to note that the change in fluorescence is the result of dATP binding to the Pol β 20/36AP complex and not the incorporation of dAMP, which occurs too slowly at the time scale of these stopped-flow experiments (1 s). These results show that, for the 19/36AP substrate, rather than observing the conversion of substrate to product, we observed the conversion of substrate to product to the ternary complex of the next mismatch at equilibrium. Nucleotide dependence assays showed a $K_{d,\text{app}}$ of $\sim 150\text{ }\mu\text{M}$ for the 2-AP \cdot A base pair (suggesting that ca. 70% of the mismatched ternary complex could exist in the conditions used), while the $K_{d,\text{app}}$ of the A \cdot A base pair was previously reported as $290\text{ }\mu\text{M}$, using a similar substrate (24). The differences in $K_{d,\text{app}}$ for 2-AP \cdot A and A \cdot A explain the difference in fluorescence between the 2-AP-containing substrate and the control substrate. This effect is not as prominent in the other substrates (ca. 10% or less of ternary complexes could be present) because the $K_{d,\text{app}}$'s of the next mismatches are substantially higher (18/36AP, T \cdot C, $630\text{ }\mu\text{M}$; 20/36AP, T \cdot T, $820\text{ }\mu\text{M}$; 21/36AP, C \cdot A, $890\text{ }\mu\text{M}$) (24).

The results of these analyses suggest that, in designing substrates and the experimental conditions for stopped-flow studies, the possibility of formation of a mismatched complex as described above should be minimized and should also be considered in the interpretation of the results. The results also suggest that the Trp fluorescence can be used as an independent probe for the conformational change of Pol β during the catalytic cycle; use of 2-AP-containing DNA is not necessary when the fluorescence of Trp is to be monitored. However, 2-AP is a more general probe since it can be placed at specific positions and since most proteins have more than one tryptophan residue that could complicate the analyses. We therefore devote the rest of the paper to analyses and interpretation of 2-AP fluorescence.

New Insight from 2-AP Fluorescence. As shown in Figure 3, the four 2-AP fluorescence curves show different shapes and different signal-to-noise ratios, much more so than the four Trp fluorescence curves. At first we considered whether the 2-AP fluorescence curve in Figure 3B was significantly influenced by the formation of mismatched ternary complexes as described in the previous section for Trp fluorescence. This appears not to be the case, since the change in the 2-AP fluorescence from the binary product complex to the mismatched ternary complex is very small (as suggested by the small amplitude of the first phase of the 2-AP curve of the 20/36AP substrate shown in Figure 3C) relative to

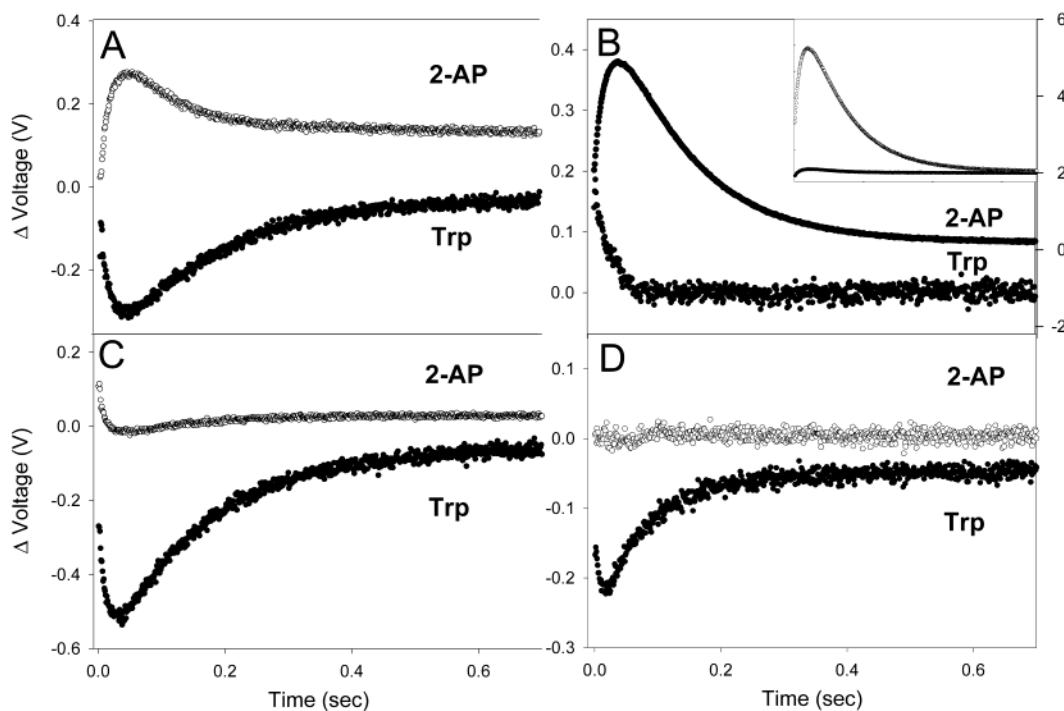
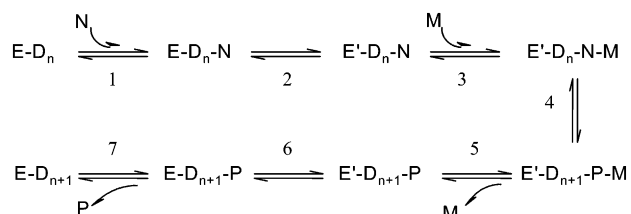


FIGURE 3: Stopped-flow fluorescence assays of various DNA substrates. The upper curves in each panel are for 2-AP fluorescence, and the lower curves are for Trp fluorescence. (A) Incorporation of dCTP into DNA substrate 18/36AP. The reactions were initiated by mixing 75 μL of each syringe. One syringe contained 800 nM 18/36AP that had been incubated with 1.6 μM Pol β and 8 mM MgCl_2 . The other syringe contained 400 μM dCTP and 8 mM MgCl_2 . (B) Incorporation of dATP into DNA substrate 19/36AP. Reaction conditions are the same as in (A). Due to the large differences in signal strength, Trp and the 2-AP signal are plotted on different Y-axes; the left axis is for Trp fluorescence, and the right axis is for 2-AP fluorescence. Inset: signal-to-noise comparison of 19/36AP and 18/36AP 2-AP fluorescence using identical conditions for each DNA substrate and presented on the same Y-axis. (C) Incorporation of TTP into DNA substrate 20/36AP. Reaction conditions are the same as in (A). (D) Incorporation of dATP into DNA substrate 21/36AP. Reaction conditions are the same as in (A).

Scheme 1^a



^a Reproduced with permission from ref 9. Copyright 2001 American Chemical Society. E = Pol β in the open finger conformation; E' = Pol β in the closed finger conformation; D = DNA; N = M·dNTP; M = catalytic metal ion; P = M·PP_i.

the large change in fluorescence associated with binary product formation shown in Figure 3B.

The next factor to consider is the effect of the location of the 2-AP probe. As shown in Figure 2B, the 2-AP probe located in different sites of DNA could experience different effects during the reaction process. The 18/36AP substrate, which places 2-AP two nucleotides downstream of the nascent base pair, will report on changes more distant from the active site. As shown in Figure 3A, it shows a biphasic emission curve similar to the previous results shown in Figure 1A but with an opposite fluorescence intensity. As shown in Figure 2B, the template position occupied by 2-AP in 19/36AP is highly distorted, with a 90° kink in the backbone. It therefore seems likely that the base at this position would experience dramatic changes in base stacking interactions during the course of a single turnover. In support of this prediction, the 19/36AP substrate yielded the greatest signal-

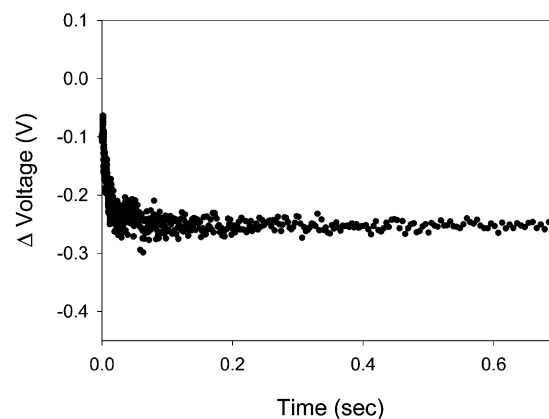


FIGURE 4: Stopped-flow fluorescence assay of dATP binding to the 20/36AP DNA substrate. The reaction was initiated by mixing 75 μL of each syringe. One syringe contained 800 nM 20/36AP that had been incubated with 1.6 μM Pol β and 8 mM MgCl_2 . The other syringe contained 400 μM dATP and 8 mM MgCl_2 . Tryptophan fluorescence was monitored as a function of time. The tryptophan emission fit best to a single exponential with a rate of $126 \pm 18 \text{ s}^{-1}$.

to-noise ratio for 2-AP fluorescence emission (Figure 3B; due to the large differences in signal intensity, Trp and 2-AP signals were plotted on different Y-axes). The inset of Figure 3B shows the enhancement of signal strength with 19/36AP vs 18/36AP; the former is nearly 20–25-fold greater than the latter. The 20/36AP substrate places 2-AP at the position opposite the incoming nucleotide. This is the substrate that has been used in all previously reported experiments using 2-AP fluorescence to study DNA polymerase reactions

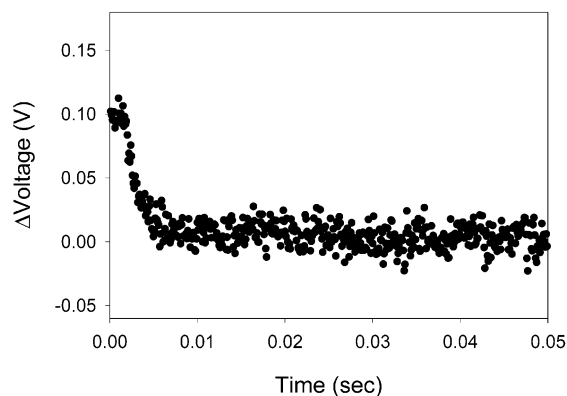


FIGURE 5: Effects of Mg^{2+} on the stopped-flow 2-AP fluorescence for the 19/36AP substrate. One syringe contained 400 nM 19/36AP preincubated with 800 nM Pol β in assay buffer at pH 8.0. The other syringe contained 16 mM $MgCl_2$ in assay buffer. The 2-AP emission fit satisfactorily to a single exponential with a rate of $460 \pm 90 \text{ s}^{-1}$.

(9, 21, 24, 25). As shown in Figure 3C, 20/36AP yields a weaker signal-to-noise ratio for 2-AP fluorescence than do 18/36AP and 19/36AP. However, the 2-AP fluorescence changes have the same direction as the Trp fluorescence changes, explaining the improvement in signal observed in our previous stopped-flow studies in which 2-AP and Trp fluorescence were partially combined. The 21/36AP substrate places 2-AP in the duplex DNA immediately upstream of the nascent base pair. In this location, in contrast to the other three examined, 2-AP undergoes no fluorescence change during the reaction, as shown in Figure 3D. This suggests that the upstream duplex DNA is relatively static and that π -stacking interactions between this base and the templating base are largely unaltered throughout the course of a single turnover.

These results show that the 19/36AP substrate is an excellent reporter under these conditions. However, this location may not be ideal for studying pyrimidine incorporation, since the next base (2-AP) can pair with pyrimidines and be rapidly incorporated (24), making it impossible to study single base incorporation. It also has limitations if Trp fluorescence is also desired. The 18/36AP substrate, however, is less sensitive but should be able to accommodate any base pair desired. It also has acceptable signal-to-noise ratios for both 2-AP and Trp fluorescence. These two DNA substrates are therefore used in additional assays in the rest of this paper.

Effects of Mg^{2+} in 2-AP Stopped-Flow Fluorescence Experiments. In this section we examine the effect of Mg^{2+} on the 2-AP fluorescence curves in stopped-flow experiments. Our studies were performed with the 18/36AP and 19/36AP substrates. We first examined the effect of Mg^{2+} in the absence of dNTP. Figure 5 shows that adding Mg^{2+} to a solution of Pol β and 19/36AP causes a fast decrease in fluorescence. A similar effect is seen with the 18/36AP substrate (data not shown). This effect was eliminated in later experiments by maintaining equal concentrations of Mg^{2+} in both syringes for the remaining experiments.

We then examined the effect of Mg^{2+} on nucleotide incorporation. As shown in Figure 6A, the 18/36AP substrate displays an unusual phenomenon in its Mg^{2+} dependence: the directions of both the fast and slow phases reverse as the Mg^{2+} concentration increases. At low Mg^{2+} concentra-

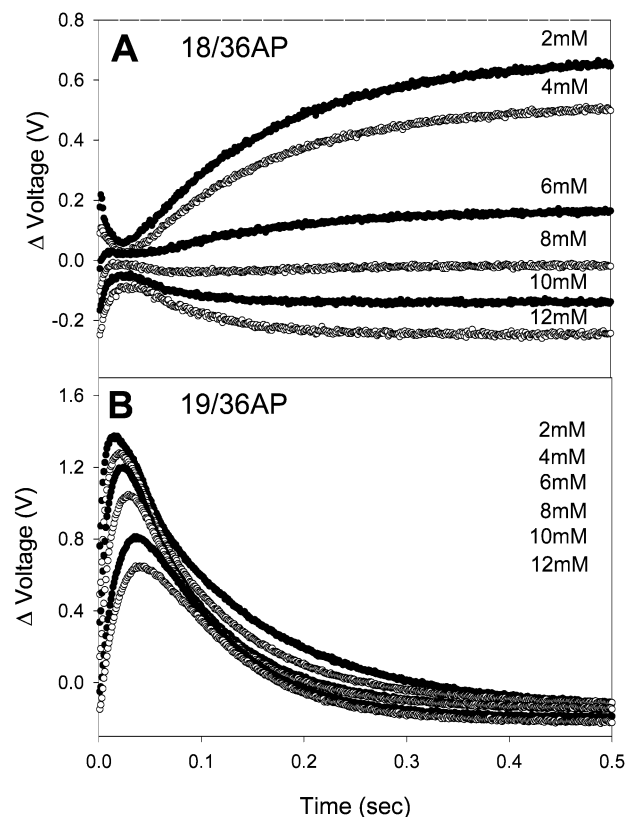


FIGURE 6: Effects of Mg^{2+} on the stopped-flow 2-AP fluorescence assay for dNTP incorporation into 18/36AP (A) and 19/36AP (B). One syringe contained Pol β [$1.6 \mu\text{M}$ in (A) and $0.8 \mu\text{M}$ in (B)] that had been incubated with DNA [800 nM in (A) and 400 nM in (B)] and a variable concentration of $MgCl_2$ in assay buffer. The other syringe contained $600 \mu\text{M}$ dCTP (A) or dATP (B) and an equivalent concentration of $MgCl_2$ in assay buffer. Each fluorescence trace is offset by ca. 0.03 unit. The fluorescence traces from top to bottom are for 2, 4, 6, 8, 10, and 12 mM $MgCl_2$ (final concentration).

tions (0–5 mM) the fast phase is decreasing and the slow phase is increasing and vice versa at higher Mg^{2+} concentrations (>5 mM). On the other hand, the 19/36AP substrate does not show a change in the direction of fluorescence with increasing [Mg^{2+}], as shown in Figure 6B. The previously studied 20/36AP substrate also does not show a change in the direction of fluorescence with increasing [Mg^{2+}] (24). These results indicate that the concentration of Mg^{2+} has a large effect on both fluorescence intensity and direction of fluorescence changes in stopped-flow analysis of the reaction catalyzed by Pol β . Furthermore, the effect of Mg^{2+} depends on the location of 2-AP in the DNA substrate used. The nature of this effect remains unresolved, and efforts are under way to determine if this effect is a result of specific or nonspecific interactions.

Further Evaluation of the “Slow Phase” Using Improved Conditions. In the rest of this paper, we report the use of the two better substrates monitored by 2-AP fluorescence to reevaluate the results obtained previously for the 20/36AP substrate monitored by a combination of Trp and 2-AP fluorescence (21, 24). This section focuses on the rate of the slow phase and its dependence on Mg^{2+} and dNTP, while the next section focuses on the fast phase.

The Mg^{2+} and dNTP dependence of the slow phase was examined via a series of stopped-flow titrations. Figure 7 shows the fluorescence traces for the nucleotide dependence

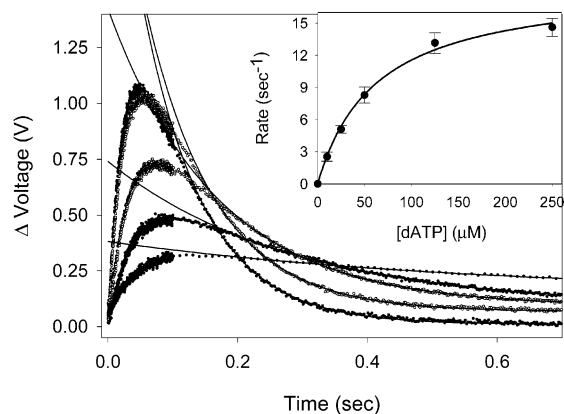


FIGURE 7: Representative nucleotide-dependent stopped-flow 2-AP fluorescence assays using the 19/36AP substrate. One syringe contained 400 nM 19/36AP preincubated with 800 nM Pol β and 8 mM MgCl₂ in assay buffer at pH 8.0. The other syringe contained 8 mM MgCl₂ and a variable amount of dATP (20, 50, 100, 250, and 500 μ M; traces are displayed from bottom to top) in assay buffer at pH 8.0. The reaction was initiated by mixing 75 μ L from both syringes. The slow phase of the fluorescence change was fit to a single-exponential equation (eq 1) as described in the text, and the resultant curves are plotted. Inset: plot of the rate of the slow phase vs dATP concentration. The data were fit to a hyperbolic equation (eq 2) and yielded a $K_{d,app}$ of $46 \pm 10 \mu$ M for dATP and a k_{max} of $15.5 \pm 2.1 \text{ s}^{-1}$.

Table 1: Summary of Kinetic Constants Obtained from Stopped-Flow and Chemical Quench Assays (pH 8.0 and 37 °C)

DNA substrate	variable	k_{max} or $k_{pol}(\text{s}^{-1})$	$K_{d,app}$
18/36AP			
stopped flow	dCTP	12.2 ± 2.1	$27 \pm 8 \mu\text{M}$
(slow phase)	Mg ²⁺	12.5 ± 1.8	$0.60 \pm 0.25 \text{ mM}$
chemical quench	dCTP	12.7 ± 1.8	$33 \pm 7 \mu\text{M}$
	Mg ²⁺	13.1 ± 3.1	$0.70 \pm 0.15 \text{ mM}$
19/36AP			
stopped flow	dATP	15.5 ± 2.1	$46 \pm 10 \mu\text{M}$
(slow phase)	Mg ²⁺	15.2 ± 2.4	$1.0 \pm 0.3 \text{ mM}$
chemical quench	dATP	15.6 ± 2.6	$42 \pm 15 \mu\text{M}$
	Mg ²⁺	16.1 ± 3.3	$0.90 \pm 0.22 \text{ mM}$

of the 19/36AP substrate. The data were analyzed by fitting the slow phase (starting times $> 6 \times \tau_{1/2}$ of the fast phase) of the stopped-flow data to a single exponential. The rate of the slow phase showed a hyperbolic dependence on both Mg²⁺ and dNTP concentration for both the 19/36AP and the 18/36AP substrates. A saturation curve was constructed by plotting rate vs [ligand], which was then fit to eq 2. An example of such fitting is shown in the inset of Figure 7. The results are summarized in Table 1. These results are comparable to those previously reported for the 20/36AP substrate, a $K_{d,app}$ of $13 \pm 2 \mu$ M for TTP and a $K_{d,app}$ of $1.4 \pm 0.2 \text{ mM}$ for the catalytic Mg²⁺ (21, 24). In the absence of Mg²⁺, no fluorescence change was observed for any substrate. The results confirm that the slow phase occurs after the formation of the ternary complex, since it shows dependence on both dNTP and Mg²⁺.

The rate of the slow phase was then compared with the k_{pol} determined by a rapid chemical quench assay for both the 18/36AP and 19/36AP substrates. Figure 8 shows representative data for the 19/36AP substrate. In Figure 8A, the rate of product formation at different dNTP concentrations was fit to a single-exponential equation (eq 1). The rate was then plotted as a function of dATP concentration

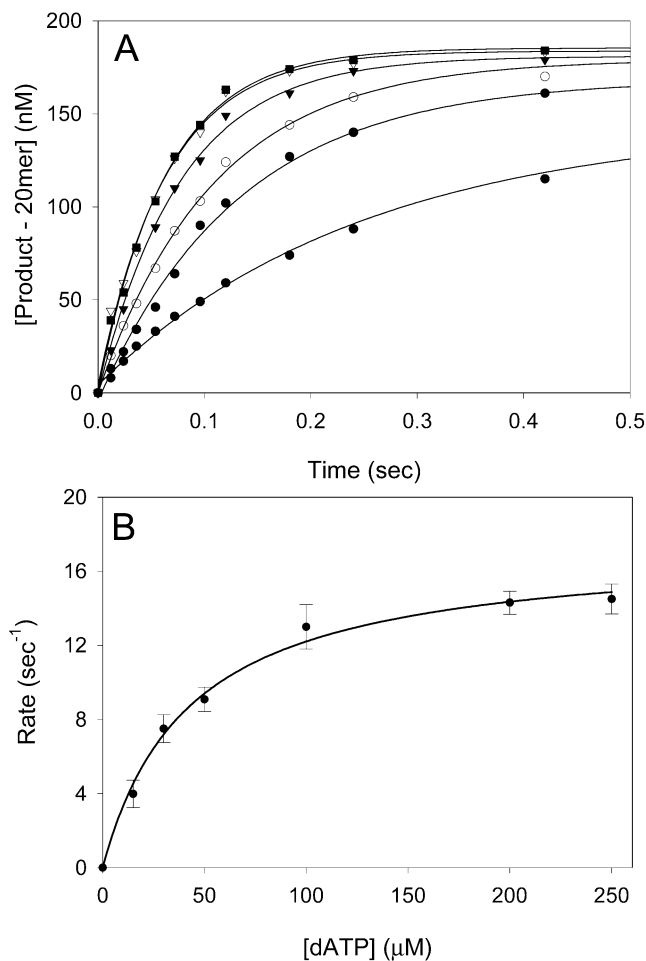


FIGURE 8: Representative nucleotide-dependent rapid chemical quench assays using the 19/36AP substrate. (A) One syringe contained 400 nM 19/36AP preincubated with 800 nM Pol β and 8 mM MgCl₂ in assay buffer at pH 8.0. The other syringe contained 8 mM MgCl₂ and a variable amount of dATP (30, 60, 100, 200, 400, and 500 μ M) in assay buffer at pH 8.0. The reaction was initiated by mixing 15 μ L from both syringes. The reaction was then quenched with 600 mM EDTA. The rate of product formation was fit to a single-exponential equation (eq 1), and the resultant curves are plotted. (B) Plot of rate vs dATP concentration. Data were fit to a hyperbolic equation (eq 2) and yielded a $K_{d,app}$ of $42 \pm 15 \mu$ M for dATP and a k_{pol} of $15.6 \pm 2.6 \text{ s}^{-1}$.

and fit to a hyperbolic equation (eq 2) as shown in Figure 8B. The results are summarized in Table 1. These results indicate that the k_{pol} values are almost identical to the corresponding maximal rates of the second phase reported in the preceding paragraph. Figure 9 shows a graphical comparison of the two results for the 19/36AP substrate. For easier comparison, the stopped-flow data were inverted and normalized to the amount of product formed in the rapid quench assay. This was accomplished by fitting the second phase (starting times $> 6 \times \tau_{1/2}$ of the fast phase) of the stopped-flow data to a single exponential (eq 1) and scaling the derived amplitude to the total amount of product formed in the rapid chemical quench assay. These results agree with our previously published results for the 20/36AP substrate, which shows that the slow phase of fluorescence changes corresponds to the rate of product formation (21, 25).

Further Evaluation of the "Fast Phase" Using Improved Conditions. In the dideoxy-terminated primer experiment reported previously for the 20dd/36AP substrate (Figure 1B),

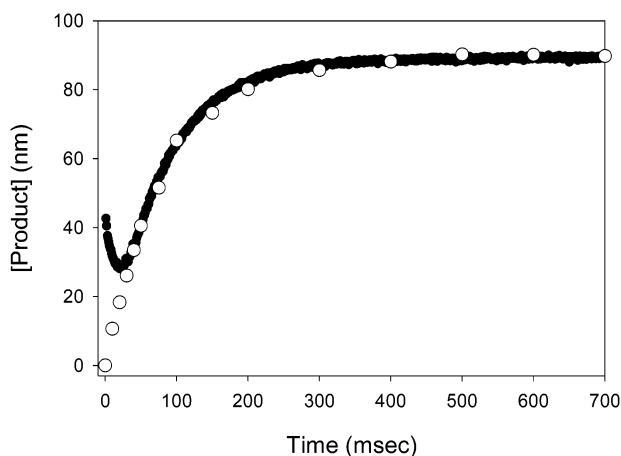


FIGURE 9: Comparison of 2-AP stopped-flow (●) and rapid chemical quench (○) assays for incorporation of dATP into the 19/36AP DNA substrate. One syringe contained 400 nM 19/36AP that had been incubated with 800 nM Pol β and 8 mM MgCl₂. The other syringe contained 400 μ M dATP and 8 mM MgCl₂.

we showed that the fast phase can be further resolved into two phases: 260 and 44 s⁻¹ (9). However, we were uncertain about its reproducibility (since the fastest phase is partly completed during the dead time of the instrument, ca. 1.8 ms). We have now performed similar experiments on the 18dd/36AP and 19dd/36AP substrates by monitoring 2AP fluorescence. The 18dd/36AP substrate was analyzed under low Mg²⁺ concentrations (3 mM), since the signal-to-noise ratio is better than at higher Mg²⁺ concentrations. Fluorescence time traces were collected for both 2-AP (315 nm excitation) and tryptophan (285 nm excitation) emission. Figure 10 shows a representative fluorescence curve with the 19/36AP substrate and monitoring 2-AP fluorescence. In both cases, the slow phase was not observed, supporting the previous interpretation that the slow phase does not represent a rate-limiting conformational change before the chemical step. For 18dd/36AP, the tryptophan emission fits well to a single-exponential equation with a rate of 96 \pm 19 s⁻¹, and the 2-AP emission fits best to a double-exponential equation with rates of 293 \pm 60 and 67 \pm 15 s⁻¹. For the 19dd/36AP DNA, the tryptophan emission fits well to a single-exponential equation with a rate of 106 \pm 33 s⁻¹, and 2-AP emission fit best to a double-exponential equation with rates of 370 \pm 30 and 66 \pm 8 s⁻¹. These results are similar to those that our laboratory previously reported for the 20dd/36AP substrate.

To further understand the nature of the two fast phases, Mg²⁺ concentration dependence was examined using the 19dd/36AP substrate. The rate of both fast phases showed no dependence on Mg²⁺ concentration (300 μ M–10 mM). These results support that the fluorescence changes of both fast phases occur before binding of the catalytic metal, since they are not affected by the binding of the catalytic metal. While previous studies have suggested that the fast phase corresponds to the domain-closing conformational change (E to E' in Scheme 1) observed in crystal structures (9), it is not known which of the two fast phases, or both of them, corresponds to this conformational change.

Stopped-Flow Study of the Reverse Reaction with 19/36AP. The reverse reaction, also known as pyrophosphorolysis, is initiated by the addition of pyrophosphate (PP_i) and Mg²⁺ to the binary complex (E·DNA). The stopped-flow fluores-

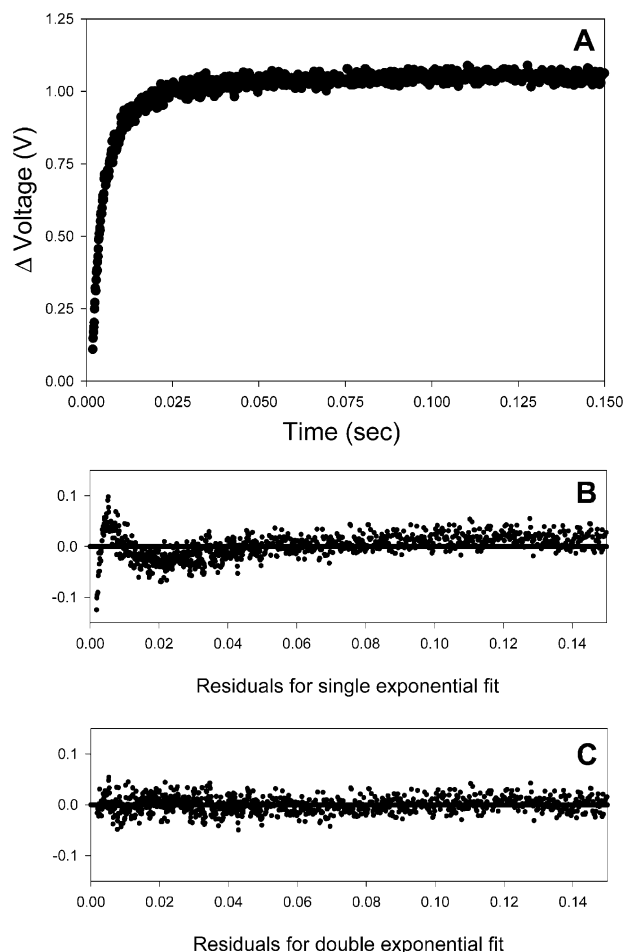


FIGURE 10: (A) Stopped-flow 2-AP fluorescence assays using a terminated primer. One syringe contained 400 nM 19dd/36AP that had been incubated with 800 nM Pol β and 8 mM MgCl₂ in assay buffer at pH 8.0. The other syringe contained 400 μ M dATP and 8 mM MgCl₂ in assay buffer at pH 8.0. The reaction was initiated by mixing 75 μ L from both syringes. The 2-AP emission fits best to a double-exponential equation with rates of 370 \pm 30 and 66 \pm 8 s⁻¹. (B) Residuals for a single-exponential fit with a rate of 190 \pm 75 s⁻¹. (C) Residuals for a double-exponential fit with rates of 370 \pm 30 and 66 \pm 8 s⁻¹.

cence of the reverse reaction has been examined previously with 21/36AP (24). In this work it was examined with 20/36AP (corresponding to 19/36AP in the forward reaction) DNA substrate, and the result is shown in Figure 11. The curve fits well to a three-exponential term equation (eq 2) and provided three rates of 47 \pm 8, 10 \pm 3, and 0.03 \pm 0.008 s⁻¹. These results agree, within a factor of 2, to the three rates reported previously (72 \pm 3.6, 6 \pm 2, and 0.062 \pm 0.002 s⁻¹, respectively). The slowest rate of fluorescence change occurs at a rate similar to that of product formation (0.04 \pm 0.01 s⁻¹), as determined by chemical quench assay (data not shown). Further studies are required to interpret the results quantitatively, particularly since multiple turnover reactions can occur for the reverse reaction. Our tentative interpretation is that the fastest phase corresponds to the E to E' conformational change in the reverse reaction, while the slowest phase corresponds to E' to E, which is limited by the chemical step. The magnitude of the fluorescence change is also smaller in the reverse reaction, suggesting a lower population of highly fluorescent species (as seen in the forward reaction).

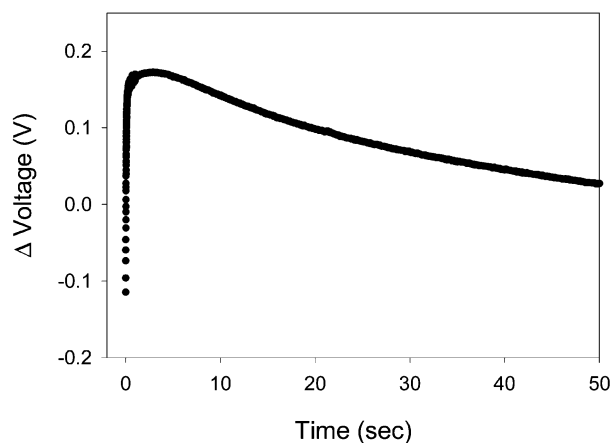


FIGURE 11: Stopped-flow fluorescence assay of the reverse reaction. One syringe contained 400 nM 20/36AP that had been incubated with 800 nM Pol β and 12 mM MgCl₂. The other syringe contained 5 mM PP_i and 12 mM MgCl₂. The 2-AP emission fits best to a triple-exponential equation with rates of 47 ± 8 , 10 ± 3 , and 0.03 ± 0.008 s⁻¹.

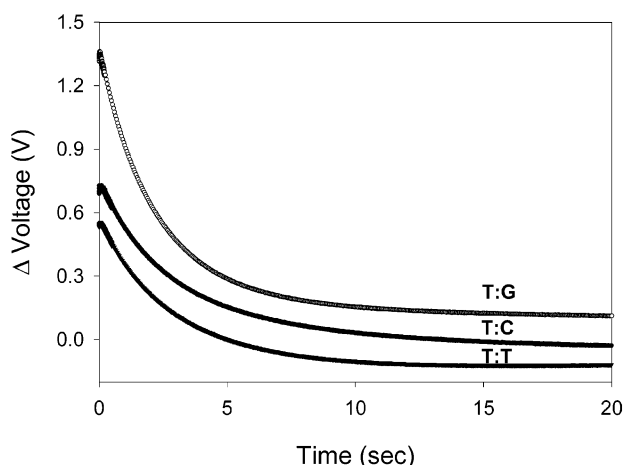


FIGURE 12: Stopped-flow fluorescence assays of the incorrect base incorporation reaction. One syringe contained 400 nM 19/36AP that had been incubated with 800 nM Pol β and 8 mM MgCl₂. The other syringe contained 2 mM appropriate dNTP and 8 mM MgCl₂. Each fluorescence profile has been offset by 0.1 unit for clarity. The 2-AP emission (points beyond 500 ms) fits best to a double-exponential equation with rates as follows: T•G, 0.52 ± 0.11 and 0.18 ± 0.04 s⁻¹; T•C, 0.32 ± 0.06 and 0.11 ± 0.03 s⁻¹; T•T, 0.48 ± 0.10 and 0.15 ± 0.04 s⁻¹.

Stopped-Flow Study of Incorrect Nucleotide Incorporation with 19/36AP. To better understand the mechanism by which Pol β discriminates against incorrect nucleotides, we investigated the stopped-flow fluorescence changes associated with incorrect nucleotide incorporation. Again, we chose the 19/36AP DNA substrate for these studies, since it has the greatest signal-to-noise ratio. The 19/36AP DNA substrate has a T in the nascent template position, so the correct nucleotide is dATP, forming the T•A base pair (template–nucleotide). Figure 12 shows the stopped-flow fluorescence changes associated with the incorporation of the three incorrect bases, G, C, and T. The results show that all of the bases induce similar fluorescence changes, which are also slightly different from those previously reported for the 20/36AP substrate (primarily based on Trp fluorescence) (24). The 20/36AP substrate showed two phases of weak fluorescence change, one very fast, ~ 250 s⁻¹, and one very slow, ~ 0.1 s⁻¹, for the 2AP•A mismatch, while the 2AP•G

mismatch had a fluorescence change too weak to interpret (24). The 19/36AP curves in Figure 12 show a very small fast phase (~ 300 s⁻¹, but only an approximate number due to the weak signal) and two very slow fluorescence changes (~ 0.4 and ~ 0.1 s⁻¹) for each incorrect nucleotide incorporation. The nature of the two very slow phases has yet to be established. It can, however, be reasonably assumed that one will reflect the rate of chemistry, since the rates are similar to those previously determined for incorrect nucleotide incorporation (41). The small amplitude of the fast phase suggests that the mismatches form a closed ternary complex with substantially reduced fluorescence, relative to the correct nucleotide. Additional experiments are required to clarify these two possibilities. In any case, our results indicate that the fast phase, which was suggested to represent the subdomain-closing conformational change (24), is perturbed in the reaction with incorrect dNTP in different ways depending on the nature of the mismatch and the DNA substrate used, while the slow phase always corresponds to the rate of the chemical step. These results fully support our notion that the fidelity of Pol β is controlled by the chemical step instead of the subdomain-closing conformational change (42).

Conclusions. The current study has expanded the scope of stopped-flow fluorescence studies of Pol β by demonstrating two independent probes to study protein and DNA conformational changes. It has also expanded the ability to study multiple base pairs with one template and has identified a series of conditions that provide improved signal-to-noise ratios and sensitivity for stopped-flow assays. The results of kinetic studies by use of the new conditions have provided further support and additional detail to the kinetic scheme shown in Scheme 1. This study also paves the way for more detailed future studies focusing on base mismatches, nucleotide analogues, site-directed mutants, and other polymerases, which will provide new insights into the mechanism of polymerase fidelity.

ACKNOWLEDGMENT

The authors thank A. K. Showalter for useful discussion and critical comment on this work.

REFERENCES

- Liu, J., and Tsai, M.-D. (2001) DNA Polymerase β : Pre-Steady-State Kinetic Analyses of dATP α -S Stereoselectivity and Alteration of the Stereoselectivity by Various Metal Ions and by Site-Directed Mutagenesis, *Biochemistry* 40, 9014–9022.
- Kunkel, T. A., and Bebenek, K. (2000) DNA replication fidelity, *Annu. Rev. Biochem.* 69, 497–529.
- Steitz, T. A. (1999) DNA polymerases: structural diversity and common mechanisms, *J. Biol. Chem.* 274, 17395–17398.
- Johnson, K. A. (1993) Conformational coupling in DNA polymerase fidelity, *Annu. Rev. Biochem.* 62, 685–713.
- Goodman, M. F. (1997) Hydrogen bonding revisited: geometric selection as a principal determinant of DNA replication fidelity, *Proc. Natl. Acad. Sci. U.S.A.* 94, 10493–10495.
- Joyce, C. M., and Steitz, T. A. (1994) Function and structure relationships in DNA polymerases, *Annu. Rev. Biochem.* 63, 777–822.
- Steitz, T. A. (1993) DNA- and RNA-dependent DNA polymerases, *Curr. Opin. Struct. Biol.* 3, 31–38.
- Pelletier, H., Sawaya, M. R., Kumar, A., Wilson, S. H., and Kraut, J. (1994) Structures of ternary complexes of rat DNA polymerase beta, a DNA template-primer, and ddCTP, *Science* 264, 1891–1903.

9. Arndt, J. W., Gong, W., Zhong, X., Showalter, A. K., Liu, J., Dunlap, C. A., Lin, Z., Paxson, C., Tsai, M. D., and Chan, M. K. (2001) Insight into the catalytic mechanism of DNA polymerase beta: structures of intermediate complexes, *Biochemistry* 40, 5368–5375.
10. Sawaya, M. R., Pelletier, H., Kumar, A., Wilson, S. H., and Kraut, J. (1994) Crystal structure of rat DNA polymerase beta: evidence for a common polymerase mechanism, *Science* 264, 1930–1935.
11. Sawaya, M. R., Prasad, R., Wilson, S. H., Kraut, J., and Pelletier, H. (1997) Crystal structures of human DNA polymerase β complexed with gapped and nicked DNA: evidence for an induced fit mechanism, *Biochemistry* 36, 11205–11215.
12. Pelletier, H., Sawaya, M. R., Wolfle, W., Wilson, S. H., and Kraut, J. (1996) Crystal structures of human DNA polymerase beta complexed with DNA: implications for catalytic mechanism, processivity, and fidelity, *Biochemistry* 35, 12742–12761.
13. Singhal, R. K., and Wilson, S. H. (1993) Short gap-filling synthesis by DNA polymerase beta is processive, *J. Biol. Chem.* 268, 15906–15911.
14. Ahn, J., Werneburg, B. G., and Tsai, M.-D. (1997) DNA Polymerase beta: Structure-Fidelity Relationship from Pre-Steady-State Kinetic Analyses of All Possible Correct and Incorrect Base Pairs for Wild-Type and R283A Mutant, *Biochemistry* 36, 1100–1107.
15. Ahn, J., Kraynov, V. S., Zhong, X., Werneburg, B. G., and Tsai, M. D. (1998) DNA polymerase beta: effects of gapped DNA substrates on dNTP specificity, fidelity, processivity and conformational changes, *Biochem. J.* 331, 79–87.
16. Beard, W. A., Osheroff, W. P., Prasad, R., Sawaya, M. R., Jaju, M., Wood, T. G., Kraut, J., Kunkel, T. A., and Wilson, S. H. (1996) Enzyme-DNA interactions required for efficient nucleotide incorporation and discrimination in human DNA polymerase beta, *J. Biol. Chem.* 271, 12141–12144.
17. Prasad, R., Beard, W. A., and Wilson, S. H. (1994) Studies of gapped DNA substrate binding by mammalian DNA polymerase beta. Dependence on 5'-phosphate group, *J. Biol. Chem.* 269, 18096–18101.
18. Clairmont, C. A., Narayanan, L., Sun, K. W., Glazer, P. M., and Sweasy, J. B. (1999) The Tyr-265-to-Cys mutator mutant of DNA polymerase beta induces a mutator phenotype in mouse LN12 cells, *Proc. Natl. Acad. Sci. U.S.A.* 96, 9580–9585.
19. Kosa, J. L., and Sweasy, J. B. (1999) The E249K mutator mutant of DNA polymerase beta extends mispaired termini, *J. Biol. Chem.* 274, 35866–35872.
20. Li, S. X., Vaccaro, J. A., and Sweasy, J. B. (1999) Involvement of phenylalanine 272 of DNA polymerase beta in discriminating between correct and incorrect deoxynucleoside triphosphates, *Biochemistry* 38, 4800–4808.
21. Shah, A. M., Li, S.-X., Anderson, K. S., and Sweasy, J. B. (2001) Y265H mutator mutant of DNA polymerase beta. Proper geometric alignment is critical for fidelity, *J. Biol. Chem.* 276, 10824–10831.
22. Vande Berg, B. J., Beard, W. A., and Wilson, S. H. (2001) DNA structure and aspartate 276 influence nucleotide binding to human DNA polymerase beta. Implication for the identity of the rate-limiting conformational change, *J. Biol. Chem.* 276, 3408–3416.
23. Werneburg, B. G., Ahn, J., Zhong, X., Hondal, R. J., Kraynov, V. S., and Tsai, M. D. (1996) DNA polymerase beta: pre-steady-state kinetic analysis and roles of arginine-283 in catalysis and fidelity, *Biochemistry* 35, 7041–7050.
24. Zhong, X., Patel, S. S., Werneburg, B. G., and Tsai, M. D. (1997) DNA polymerase β : multiple conformational changes in the mechanism of catalysis, *Biochemistry* 36, 11891–11900.
25. Zhong, X., Patel, S. S., and Tsai, M.-D. (1998) DNA Polymerase β . 5. Dissecting the Functional Roles of the Two Metal Ions with Cr(III)dTTP, *J. Am. Chem. Soc.* 120, 235–236.
26. Frey, M. W., Sowers, L. C., Millar, D. P., and Benkovic, S. J. (1995) The nucleotide analogue 2-aminopurine as a spectroscopic probe of nucleotide incorporation by the Klenow fragment of *Escherichia coli* polymerase I and bacteriophage T4 DNA polymerase, *Biochemistry* 34, 9185–9192.
27. Ward, D. C., Reich, E., and Stryer, L. (1969) Fluorescence studies of nucleotides and polynucleotides. I. Formycin, 2-aminopurine riboside, 2,6-diaminopurine riboside, and their derivatives, *J. Biol. Chem.* 244, 1228–1237.
28. Bloom, L. B., Otto, M. R., Eritja, R., Reha-Krantz, L. J., Goodman, M. F., and Beechem, J. M. (1994) Pre-Steady-State Kinetic Analysis of Sequence-Dependent Nucleotide Excision by the 3'-Exonuclease Activity of Bacteriophage T4 DNA Polymerase, *Biochemistry* 33, 7576–7586.
29. Bandwar, R. P., and Patel, S. S. (2001) Peculiar 2-aminopurine fluorescence monitors the dynamics of open complex formation by bacteriophage T7 RNA polymerase, *J. Biol. Chem.* 276, 14075–14082.
30. Singh, I., Hecker, W., Prasad, A. K., Parmar, V. S., and Seitz, O. (2002) Local disruption of DNA-base stacking by bulky base surrogates, *Chem. Commun.*, 500–501.
31. Mandal, S. S., Fidalgo da Silva, E., and Reha-Krantz, L. J. (2002) Using 2-aminopurine fluorescence to detect base unstacking in the template strand during nucleotide incorporation by the bacteriophage T4 DNA polymerase, *Biochemistry* 41, 4399–4406.
32. Rachofsky, E. L., Osman, R., and Ross, J. B. A. (2001) Probing Structure and Dynamics of DNA with 2-Aminopurine: Effects of Local Environment on Fluorescence, *Biochemistry* 40, 946–956.
33. Larsen, O. F. A., Van Stokkum, I. H. M., Gobets, B., Van Grondelle, R., and Van Amerongen, H. (2001) Probing the structure and dynamics of a DNA hairpin by ultrafast quenching and fluorescence depolarization, *Biophys. J.* 81, 1115–1126.
34. Jean, J. M., and Hall, K. B. (2001) 2-Aminopurine fluorescence quenching and lifetimes: role of base stacking, *Proc. Natl. Acad. Sci. U.S.A.* 98, 37–41.
35. Casas-Finet, J. R., Kumar, A., Morris, G., Wilson, S. H., and Karpel, R. L. (1991) Spectroscopic studies of the structural domains of mammalian DNA beta-polymerase, *J. Biol. Chem.* 266, 19618–19625.
36. Merrill, C. R., Dunau, M. L., and Goldman, D. (1981) A rapid sensitive silver stain for polypeptides in polyacrylamide gels, *Anal. Biochem.* 110, 201–207.
37. Warshaw, M. M., and Cantor, C. R. (1970) Oligonucleotide interactions. IV. Conformational differences between deoxy- and ribodinucleoside phosphates, *Biopolymers* 9, 1079–1103.
38. Jezewska, M. J., Rajendran, S., and Bujalowski, W. (2001) Energetics and specificity of rat DNA polymerase.beta. interactions with template-primer and gapped DNA substrates, *J. Biol. Chem.* 276, 16123–16136.
39. Tsoi, P. Y., and Yang, M. (2002) Kinetic study of various binding modes between human DNA polymerase beta and different DNA substrates by surface-plasmon-resonance biosensor, *Biochem. J.* 361, 317–325.
40. Steitz, T. A., Smerdon, S. J., Jager, J., and Joyce, C. M. (1994) A unified polymerase mechanism for nonhomologous DNA and RNA polymerases, *Science* 266, 2022–2025.
41. Ahn, J., Werneburg, B. G., and Tsai, M. D. (1997) DNA polymerase beta: structure-fidelity relationship from Pre-steady-state kinetic analyses of all possible correct and incorrect base pairs for wild type and R283A mutant, *Biochemistry* 36, 1100–1107.
42. Showalter, A. K., and Tsai, M. D. (2002) Reexamination of the Nucleotide Incorporation Fidelity of DNA Polymerases, *Biochemistry* 41, 10571–10576.

BI025837G